Radiative Penguin Decays from BABAR

G Eigen (representing the BABAR collaboration)

Department of Physics, University of Bergen

We summarize the latest BABAR results on $B \to K^{(*)}\ell^+\ell^-$ and $B \to \rho(\omega)\gamma$.

1 Introduction

Electroweak penguin decays provide a promising hunting ground for Physics beyond the Standard Model (SM). The decay $B \to X_s\gamma$, which proceeds through an electromagnetic penguin loop, already provides stringent constraints on the supersymmetric (SUSY) parameter space [1]. The present data samples of $\sim 1 \times 10^8 B\bar{B}$ events allow to explore radiative penguin decays with branching fractions of the order of 10^{-6} or less. In this brief report we discuss a study of $B \to K^{(*)}\ell^+\ell^-$ decay modes and a search for $B \to \rho(\omega)\gamma$ decays.

2 Study of $B \to K\ell^+\ell^-$ and $B \to K^*\ell^+\ell^-$

The decays $B \to K\ell^+\ell^-$ and $B \to K^*\ell^+\ell^-$ proceed through an electromagnetic penguin loop, a Z^0 penguin loop or a weak box diagram as shown in Figure 1. In the operator product expansion (OPE) the decay rate is factorized into perturbatively calculable short-distance contributions that are parameterized by scale-dependent Wilson coefficients and non-perturbative long-distance effects that are represented by local four-quark operators. Operator mixing occurring in next-to-leading order perturbation theory leads to three effective scale-dependent Wilson coefficients, $C_7^{eff}(\mu_b)$, $C_9^{eff}(\mu_b)$, and $C_{10}^{eff}(\mu_b)$ that are each sensitive to New Physics contributions. Examples for non-SM penguin loops are depicted in Figure 2. In the Standard Model the branching fractions are predicted to be within the following ranges, $\mathcal{B}(B \to K\ell^+\ell^-) = (0.24\text{–}0.97)\times 10^{-6}$, $\mathcal{B}(B \to K^*\mu^+\mu^-) = (0.8 - 2.64) \times 10^{-6}$ and $\mathcal{B}(B \to K^*e^+e^-) = (1.09 - 2.66) \times 10^{-6}$ [2]. In supersymmetric models, for example, the branching fractions my be enhanced by more than a factor of two [1].

BABAR has analyzed eight final states where a $K^\pm, K^0_S, K^{*0}$ or $K^{*\pm}$ recoils against a $\mu^+\mu^-$ or e^+e^- pair, using an integrated luminosity of 77.8 fb^{-1} that corresponds to $(84.4 \pm 0.9) \times 10^6$ $B\bar{B}$ events. The discriminating variables are beam energy-substituted mass $m_{ES} = \sqrt{(E^*_{beam})^2 - (\vec{p}^*_B)^2}$ and the energy difference $\Delta E = E^*_B - E^*_{beam}$, where $\vec{p}_B$, E_B and E_{beam} denote the B-momentum, B-energy and beam energy in the center-of-mass (CM) frame, respectively. The $\Delta E - m_{ES}$ *plane*

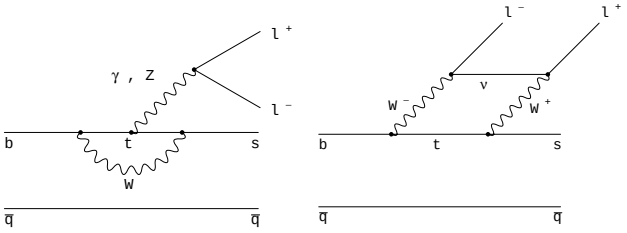

Figure 1. Lowest-order diagrams for $B \to K^{(*)}\ell^+\ell^-$ in SM.

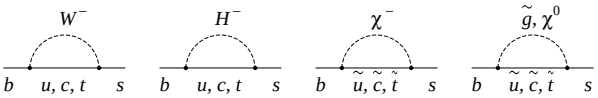

Figure 2. Penguin loop diagrams involving a W boson, a charged Higgs boson, a chargino and a neutralino (gluino), respectively.

is devided into three regions, a signal region ($\pm 3\sigma$ boxes around the signal), the fit region ($m_{ES} > 5.2$ GeV, $|\Delta E^*| < 250$ MeV), and a large side band ($m_{ES} > 5.0$ GeV, $|\Delta E^*| < 500$ MeV). Specific selection criteria are used to suppress individual backgrounds. A Fisher discriminant [5], which is based on the thrust angle between the daughter particles of the B-Meson candidate and that of the remaining particles in the event ($\cos\theta_T$), the B decay angle in the $\Upsilon(4S)$ rest frame between the B candidate and the beam axis ($\cos\theta^*_B$), the ratio of second-to-zeroth Fox-Wolfram moments, R_2 [3], and the invariant mass of the $K - \ell$ system $m_{k\ell}$, is used to eliminate the back-to-back continuum background. To discriminate against combinatorial $B\bar{B}$ background a likelihood function is used that combines the missing energy in the event (E_{miss}), with the dilepton vertex probability, the significance of the dilepton separation along the beam direction and $\cos\theta^*_B$. To reject events from $B \to J/\psi K^{(*)}$ and $B \to \psi(2S)K^{(*)}$ decays with $J/\psi(\psi(2S) \to \ell^+\ell^-$ that have the same event toplogies in a restricted $m_{\ell\ell}$ mass region as signal events, the shaded regions in the $\Delta E - m_{\ell\ell}$ plane shown in Figure 3 are vetoed. The inclined bands provide an efficient rejection of $J/\psi K^{(*)}$ events in the fit region, in which one or both leptons radiated a photon.

The selection criteria are optimized on simulated data as

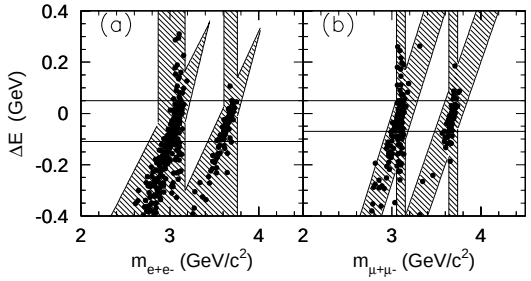

Figure 3. Charmonium veto (hatched regions) in the $\Delta E^* - m_{\ell^+\ell^-}$ plane for a) $B \to K^{(*)}e^+e^-$ and b) $B \to K^{(*)}\mu^+\mu^-$. The dots represent simulations for $B \to J/\psi(\to \ell^+\ell^-)K^{(*)}$ and $B \to \psi(2S)(\to \ell^+\ell^-)K^{(*)}$.

well as data sidebands. While simulated data are used to determine efficiencies and estimate peaking backgrounds, the Monte Carlo results are checked using data control samples, including both exclusive and inclusive charmonium decays, $B \to D\pi$ decays, data sidebands and $K^{(*)}e^\pm\mu^\mp$ samples. For the exclusive charmonium modes an excellent data/Monte Carlo agreement of 1.015 ± 0.019 is obtained. Further details of the event selection are discussed in [6]. In each of the eight final states, a signal is extracted from a two-dimensional fit to the $m_{ES} - \Delta E$ plane. The signal shapes are obtained from Monte Carlo samples with fine-tuning on the exclusive charmonium modes. To account for radiation effects and correlations between ΔE and M_{ES} a product of Crystal Ball functions is used [7]. The combinatorial backgrounds are parameterized with ARGUS functions [8], where both the normalization and the shape parameters are left free. Only in $B \to K^\pm e^+e^-$, a significant yield of $14.4^{+5.0}_{-4.2}$ events is observed. The selection efficiency is 17.5%, yielding a branching fraction of

$$\mathcal{B}(B^+ \to K^+e^+e^-) = (0.98^{+0.34+0.16}_{-0.28-0.22}) \times 10^{-6} \quad (1)$$

The second largest yield of $(10.6^{+5.2}_{-4.3})$ events is found for $B^0 \to K^{*0}e^+e^-$ for which a selection efficiency of 10.6% is achieved. The individual results for each of the eight final states are summarized in Table 1.

The M_{ES} and ΔE distributions for $B \to K\ell^+\ell^-$ and $B \to K^*\ell^+\ell^-$ summed over all individual final states are shown in Figure 4. In order to combine $K^*\mu^+\mu^-$ and $K^*e^+e^-$ results their ratio of branching fractions is assumed to be $\mathcal{B}(B \to K^*e^+e^-)/\mathcal{B}(B \to K^*\mu^+\mu^-) = 1.21$ [1]. The multiplicative systematic errors range from 7% – 8% for $K\ell^+\ell^-$ modes and 7% – 11% for $K^*\ell^+\ell^-$ modes. The largest contributions result from the model dependence (4%–7%), e/μ identification (2.7%/2.0%), K/π identification (2%–4%), K^0_S identification (3.2%), $B\bar{B}$ likelihood ratio (2.5%), and the tracking efficiency for hadrons/leptons (1.3% – 3.9%/1.6%). Contributions from the Fisher discriminant, Monte Carlo statistics and $B\bar{B}$ counting are small (< 2%). The additive systematic errors result from the signal yields in the fit, including uncertainties in signal shapes, background shapes and the amount of peaking backgrounds. The significance of the combined $K\ell^+\ell^-$ sample is 4.4σ including all systematic errors, while that of the combined $K^*\ell^+\ell^-$ sample is 2.8σ. For the combined $B \to K\ell^+\ell^-$ modes we measure a branching fraction of

$$\mathcal{B}(B \to Ke^+e^-) = (0.78^{+0.24+0.11}_{-0.20-0.18}) \times 10^{-6}. \quad (2)$$

For the combined $B \to K^*\ell^+\ell^-$ modes we set a branching fraction upper limit @ 90% confidence level (CL) of

$$\mathcal{B}(B^+ \to K^*e^+e^-) < \times 10^{-6}. \quad (3)$$

The BABAR results are consistent with those obtained by BELLE [9] and most SM predictions, but $\mathcal{B}(B \to K\ell^+\ell^-)$ is higher than the recent prediction by Ali *et al*.[1].

Table 1. Measured event yields, efficiencies and branching fractions for $B \to K\ell^+\ell^-$ and $B \to K^*\ell^+\ell^-$ modes

Mode	Y [events]	ϵ[%]	$\mathcal{B} \times 10^6$
$B^+ \to K^+e^+e^-$	$14.4^{+5.0}_{-4.2}$	17.5 ± 1.2	$0.98^{+0.34+0.16}_{-0.28-0.22}$
$B^+ \to K^+\mu^+\mu^-$	$0.5^{+2.3}_{-1.3}$	9.2 ± 0.6	$0.06^{+0.30+0.09}_{-0.17-0.08}$
$B^0 \to K^0e^+e^-$	$1.3^{+2.6}_{-1.7}$	18.6 ± 1.5	$0.24^{+0.49+0.09}_{-0.32-0.15}$
$B^0 \to K^0\mu^+\mu^-$	$3.6^{+2.9}_{-2.1}$	9.4 ± 0.7	$1.33^{+1.07}_{-0.78} \pm 0.26$
$B^0 \to K^{*0}e^+e^-$	$10.6^{+5.2}_{-4.3}$	10.6 ± 0.8	$1.78^{+0.87+0.48}_{-0.72-0.49}$
$B^0 \to K^{*0}\mu^+\mu^-$	$3.4^{+3.9}_{-2.8}$	6.1 ± 0.6	$0.99^{+1.14+}_{-0.82} \pm 0.39$
$B^+ \to K^{*+}e^+e^-$	$0.3^{+3.7}_{-2.3}$	10.3 ± 1.0	$0.15^{+1.87+0.69}_{-1.16-0.72}$
$B^+ \to K^{*+}\mu^+\mu^-$	$3.6^{+3.9}_{-2.5}$	5.2 ± 0.6	$3.61^{+3.91}_{-2.51} \pm 1.84$

3 Search for $B \to \rho(\omega)\gamma$

The decays $B \to \rho(\omega)\gamma$ are flavor-changing neutral $b \to d$ transitions that are mediated by an electromagnetic penguin loop and are suppressed with respect to $B \to K^*\gamma$ by $|V_{td}/V_{ts}|^2$. Thus, measuring the ratio of decay rates, $\Gamma(B \to \rho\gamma)/\Gamma(B \to K^*\gamma)$, allows us to extract $|V_{td}/V_{ts}|$. In SM the branching fraction for the charged mode in next-to-leading order is predicted to lie between $\mathcal{B}(B^+ \to \rho^+\gamma) = (0.85 \pm 0.4) \times 10^{-6}$ [10] and $\mathcal{B}(B \to \rho^+\gamma) = (1.58^{+0.53}_{-0.46}) \times 10^{-6}$ [13]. For the neutral modes the branching fractions are a factor of two smaller than that for $B^+ \to \rho^+\gamma$ due to isospin. The next-to-leading order effects are mass scale-dependent and are larger for $B \to K^{*0}\gamma$ than for $B \to \rho^+\gamma$ [10]. The decay rate depends on the effective Wilson coefficient C_7^{eff} that may be enhanced by New Physics contributions.

BABAR has searched for $B \to \rho(\omega)\gamma$ modes using an integrated luminosity of 77.8 fb^{-1} on the $\Upsilon(4S)$ peak and 9.6 fb^{-1} in the continuum 40 MeV below the $\Upsilon(4S)$ peak. Challenges in the analysis stem from a huge $q\bar{q}$ continuum background including initial-state radiation, background from $B \to K^*\gamma$ and the fact that the ρ resonance is much

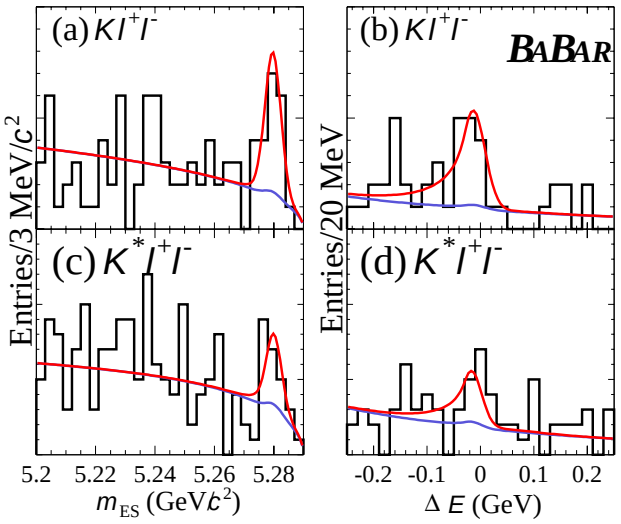

Figure 4. The m_{ES} and ΔE^* projections of the combined fits summed for the four $B \to K\ell^+\ell^-$ and the four $B \to K^*\ell^+\ell^-$ modes.

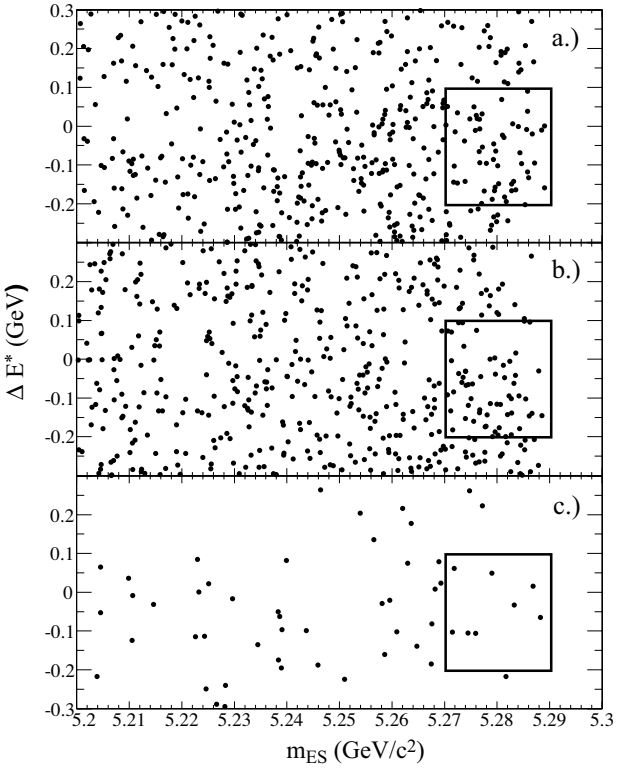

Figure 5. $\Delta E - m_{ES}$ scatter plots of the fit region for a) $B^+ \to \rho^+\gamma$, b) $B^0 \to \rho^0\gamma$ and c) $B^0 \to \omega\gamma$ candidates. The boxes indicate the expected signal regions

broader than the K^* resonance. The $q\bar{q}\gamma$ continuum background with a hard γ from initial-state radiation may have a similar event shape as that of the signal which is less spherical than a typical $B\bar{B}$ event. Photon candidates with energies of 1.5 GeV $<$ E$_\gamma$ $<$ 3.5 GeV that are inconsistent with originating from a π^0 or η decay are combined with a ρ^+, ρ^0, or ω candidate, where the latter are reconstructed from $\pi^+\pi^0$, $\pi^+\pi^-$ and three-pion combinations, respectively. Rejecting charged tracks in the signal that are consistent with a kaon, the K/π misidentification is less than 1%. The $\pi\pi$ (3π) invariant mass has to lie within a $520-1020\,\mathrm{MeV/c^2}$ ($759.6-805.6\,\mathrm{MeV/c^2}$) mass window and its momentum in the CM frame must satisfy $2.3 < \mathrm{p}^*_{\pi\pi} < 2.85$ GeV/c ($2.4 < \mathrm{p}^*_{3\pi} < 2.8$ GeV/c). A π^0 candidate must have a $\gamma\gamma$ invariant mass of $115 < \mathrm{m}_{\gamma\gamma} < 150\ \mathrm{MeV/c^2}$. To improve the momentum resolution we perform a kinematic fit with $m_{\gamma\gamma}$ constrained to the nominal π^0 mass.

To reduce the $q\bar{q}$ continuum background a neural network is used that is based on event-shape variables ($\cos\theta_{thrust}$, $\cos\theta^*_B$, $\cos\theta_{helicity}$, the Dalitz decay angle for ω, the energy flow in 18 cones around photon direction, the vertex separation Δz, the ratio of second-to-zeroth Fox Wolfram moment, R'_2, calculated in a frame recoiling the photon and the net flavor in the event [11]. The neural network is trained with Monte Carlo signal events and continuum data. The neural network output is cross-checked on the data using $B^0 \to D^-\pi^+$ that has a similar topology as the signal and $q\bar{q}$ off-resonance data. Further details of the event selection are discussed in [12].

The $\Delta E^* - m_{ES}$ distributions for the final data samples are shown in Figure 5. The signal yields are extracted from a maximum likelihood fit in the three-dimensional space $\Delta E^* - m_{ES} - m_\rho(m_\omega)$. The procedure is crosschecked with the $B \to K^*\gamma$ sample. For $B \to K^{*0}$ (K^{*+})γ the fit yields 343.2 ± 21.0 (93.1 ± 12.6) events compared to expected yields of 332 ± 36 (105 ± 18) events, respectively.

The extracted signal yields of $4.8^{+5.2}_{-4.7}$ events for $B \to \rho^0\gamma$, $6.2^{+7.2}_{-6.2}$ events for $B \to \rho^+\gamma$, and $0.1^{+2.7}_{-2.0}$ events for $B \to \omega\gamma$ are consistent with background. The efficiencies are 12.3%, 9.2% and 4.6%, respectively. Including systematic errors, which respectively increase from 11.8% to 13.4% and 17.3%, we obtain branching fraction upper limits @ 90% CL of $\mathcal{B}(B^0 \to \rho^0\gamma) < 1.2 \times 10^{-6}$, $\mathcal{B}(B^+ \to \rho^+\gamma) < 2.1 \times 10^{-6}$, and $\mathcal{B}(B^0 \to \omega\gamma) < 1.0 \times 10^{-6}$. These limits are significantly lower than those of previous searches [16][17].

Assuming isospin symmetry the $\rho^+\gamma$ and $\rho^0\gamma$ samples are combined yielding $\mathcal{B}(B \to \rho\gamma) < 1.9 \times 10^{-6}$. Using the recent BABAR $B \to K^*\gamma$ branching fraction measurement [14] this translates into an upper limit on the ratio of branching fractions of $\mathcal{B}(B \to \rho\gamma)/\mathcal{B}(B \to K^*\gamma) < 0.047$ @ 90% CL. To constrain the ratio of $|V_{td}/V_{ts}|$ we use the

Table 2. Extrapolations of the significance, experimental error on the branching fraction and experimental error on $|V_{td}/V_{ts}$ for the combined $B \to \rho(\omega)\gamma$ modes expected for different luminosities.

Luminosity	significance	$(\sigma_{\mathcal{B}}/\mathcal{B})_{exp}$	$\sigma(V_{td}/V_{ts})$
100 fb^{-1}	1.9 – 2.8 σ	0.38-0.53	0.19-0.27
200 fb^{-1}	2.7 – 3.9 σ	0.28-0.38	0.14-0.19
300 fb^{-1}	3.3 – 4.8 σ	0.23-0.31	0.12-0.15
400 fb^{-1}	3.9 – 5.5 σ	0.20-0.27	0.1-0.14
500 fb^{-1}	4.3 – 6.2 σ	0.18-0.25	0.09-0.13
1000 fb^{-1}	6.0 – 8.7 σ	0.14-0.18	0.07-0.09

parameterization [13] [15].

$$\frac{\mathcal{B}(B \to \rho\gamma)}{\mathcal{B}(B \to K^*\gamma)}) = \left|\frac{V_{td}}{V_{ts}}\right|^2 \left(\frac{1 - m_\rho^2/M_B^2}{1 - m_{K^*}^2/M_B^2}\right)^3 \zeta^2[1 + \Delta R]. \qquad (4)$$

The parameter ζ represents $SU(3)$ breaking while ΔR accounts for the annihilation diagram in $B^+ \to \rho^+\gamma$. Using $\zeta = 0.76 \pm 0.1$ and $\Delta R = 0.0 \pm 0.2$ [13] we obtain an upper limit of $|V_{td}/V_{ts}| < 0.34$ @ 90% CL. This is still larger than the limit of $|V_{td}/V_{ts}| < 0.23$ @ 95% CL which is derived from $B_s\bar{B}_s$ and $B_d\bar{B}_d$ mixing results for $\Delta m_{B_d} = 0.503 \pm 0.006$ ps^{-1}, $\Delta m_{B_s} > 14.4$ ps^{-1} @ 95% CL and $\xi = 1.24$ [4].

The present upper limits are approaching the theoretical predictions. Assumimg a branching fraction of $\mathcal{B}(B^+ \to \rho^+\gamma) = 1 \times 10^{-6}$ and $\mathcal{B}(B^0 \to \rho^0\gamma = \mathcal{B}(B \to \omega\gamma = \frac{1}{2}\mathcal{B}(B^+ \to \rho^+\gamma)$ we estimate a signal significance and experimental errors for different luminosities as listed in Table 2. The small values for the significance (*i.e.* large experimental errors on the branching fraction and on $|V_{td}/V_{ts}|$) result from the present event selection, while the large (small) values are obtained by assuming that for the same selection efficiency as in the present analysis the background is halfed. For a luminosity of $\sim 500\ fb^{-1}$ a significant measurement of these modes is expected. The limiting factor for extracting $|V_{td}/V_{ts}|$ is the theoretical uncertainty from $SU(3)$ breaking and the size of the annihilation diagram. The latter uncertainty can be removed by using only $B^0 \to \rho^)\gamma$ events, but for the same significance a factor of four increase in luminosity is required.

4 Outlook

By 2007 BABAR expects to record an integrated luminosity of ~ 500 fb^{-1}. This sample will be sufficient to measure the $B \to K^{(*)}\ell^+\ell^-$ and $B \to \rho(\omega)\gamma$ branching fractions with reasonable precision. Due to the theoretical uncertainties, however, tests of the Standard Model will be rather limited. Observables that are barely affected by theoretical uncertainties and, therefore, provide excellent tests of the Standard Model are the lepton forward-backward asymmetry as a function of $m_{\ell\ell}$ measured in $B \to K^{(*)}\ell^+\ell^-$ modes and direct CP violation in $B \to \rho gamma$ channels. In SM the the lepton forward-backward asymmetry in the B rest frame for dilepton masses below the J/ψ has a characteristic shape, crossing zero at a specfic dilepton mass [1]. The zero point is predicted in SM with small uncertainties. With limited statistics we will just determine the zero point, while with high statistics we will measure the entire distribution. Deviations from the SM shape will hint to New Physics. In SM CP asymmetries in $B \to \rho\gamma$ could be as large as 12%, but may be modified considerably in models with minimal flavor violation [13]. Precise measurements of the shape of the lepton forward-backward asymmetry and direct CP violation in $B \to \rho\gamma$, however, require data samples that are several tens of ab^{-1}.

References

1. A. Ali *et al.*, Phys. Rev. **D66**, 034002 (2002).
2. P. Colangelo *et al.*, Phys.Rev. **D53**, 3672 (1996), Erratum-ibid. **D57**, 3186 (1998); D. Melikhov *et al.*, Phys.Rev. **D57**, 6814 (1998); C.Q. Geng and C.P. Kao, Phys.Rev. **D54**, 5636 (1996); T.M. Aliev *et al.*, Phys.Lett. **B400**, 194 (1997); A. Ali *et al.*, Phys.Rev. **D61**, 074024 (2000); A. Faessler *et al.*, Eur.Phys.J.direct **C4**,18 (2002); M. Zhong *et al.*, Int.J.Mod.Phys. **A18** 1959 (2003).
3. G.C. Fox and S. Wolfram, Phys. Rev. **Lett. 41**, 1581 (1978).
4. K. Hagiwara *et al.* (Particle Data Group) Phys. Rev. **D66**, 010001 (2002).
5. R.A. Fisher, Ann. Eugenics **7** (1936).
6. B. Aubert *et al.* (BABAR collaboration), SLAC-PUB-9323, 33 pp (Jul 2002).
7. T. Skwarnicki, DESY internal report No DESY-F31-86-02 (1986); T. Skwarnicki *et al.* (Crystal Ball collaboration) Phys. Rev Lett. **58**, 972 (1987).
8. H. Albrecht *et al.* (ARGUS collaboration), Phys. Lett. **B241**, 278 (1990).
9. K. Abe *et al.* (BELLE collaboration), Phys. Rev. Lett. **88**, 021801 (2002).
10. S.W. Bosch and G. Buchalla, Nucl. Phys. **B621**, 459 (2002).
11. B. Aubert *et al.* (BABAR collaboration), Phys. Rev **D66**, 032003 (2002).
12. B. Aubert *et al.* (BABAR collaboration), SLAC-PUB-9319, 17 pp (Jul 2002).
13. A. Ali and A. Y. Parkhamenko, Eur. Phys. J. C23, 89 (2001).
14. B. Aubert *et al.* (BABAR collaboration), Phys. Rev Lett. **88**, 101805 (2002).
15. B. Grinstein and D. Pirjol, Phys. Rev. D 62, 093002 (2000).
16. T.E. Coan *et al.* (CLEO collaboration), Phys.Rev. Lett. **84**, 5283 (2000).
17. Y. Ushiroda *et al.* (BELLE collaboration), contributed to BCP4, Ise-Shima, Japan, hep-ex/0101015 (2001).